Confined states in lens-shaped quantum dots

2002 J. Phys.: Condens. Matter 14 13667

(http://iopscience.iop.org/0953-8984/14/49/321)

INSTITUTE OF PHYSICS PUBLISHING JOURNAL OF PHYSICS: CONDENSED MATTER

J. Phys.: Condens. Matter **14** (2002) 13667–13678 PII: S0953-8984(02)53379-8

Confined states in lens-shaped quantum dots

L C Lew Yan Voon[1] **and M Willatzen**[2]

[1] Department of Physics, Worcester Polytechnic Institute, 100 Institute Road, Worcester, MA 01609, USA
[2] Mads Clausen Institute, University of Southern Denmark, Grundtvigs Alle 150, DK-6400 Sønderborg, Denmark

Received 12 September 2002
Published 29 November 2002
Online at stacks.iop.org/JPhysCM/14/13667

Abstract

We solve the problem of infinite-barrier lens-shaped quantum dots (QDs) in parabolic rotational coordinates exactly. The solutions are obtained directly using the Frobenius method and also by first transforming the separated differential equations into the Whittaker equation. We have obtained a new relation connecting the Bessel wavefunctions to the Whittaker functions. Results are given for both symmetrical and asymmetrical QDs. Studies of the energy spectra at constant volume were also performed; it is found that the shape dependence is very different from those found in previous studies of QDs with ellipsoidal and elliptic shapes.

(Some figures in this article are in colour only in the electronic version)

1. Introduction

The study of semiconductor quantum dots (QDs) has always been of great interest [1]. A driving force has been the attainment of atomic-like discrete energy levels for the electrons, as opposed to the Bloch energy bands in crystals. In addition to using the QDs as model systems for investigating interesting physics such as Hund's rules and the Kondo effect, applications have been proposed (and in some cases already realized) in lasers and photodetectors, and for quantum computing and spintronics. Two directions in research can be identified. One involves numerically solving the multi-band theory of the electron in realistic shapes such as pyramidal QDs [2]. The other involves obtaining analytic or semi-analytic results for various QD shapes of somewhat higher symmetry. The latter is often done using an infinite barrier and within a one-band effective-mass approach. The goal of the latter approach is to obtain a more physical picture of the role of the shape on the electronic properties. As a recent example of use of the latter methodology, Cantele *et al* [3] discovered topological surface states in spheroidal QDs. Some of the other shapes considered so far are spheres [4], cones [5], rectangles [6], discs or cylinders [7], and domes or flat lenses [8].

This paper is motivated by the recent work of Cantele *et al* [3] in which a spheroidal QD is studied using prolate/oblate spheroidal coordinates. It was stated that the problem in the

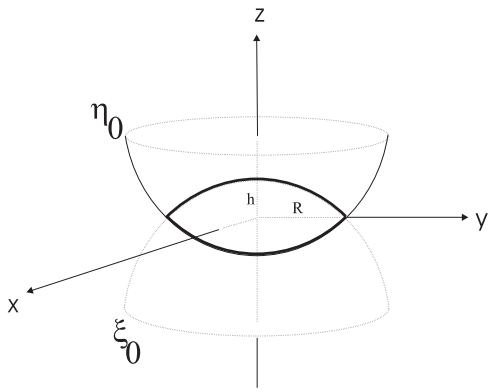

Figure 1. The lens-shaped QD in PRC.

latter coordinate system is more difficult than that of the sphere in spherical polar coordinates because of the presence of an extra separation constant in the separated ordinary differential equations (in addition to the energy, equation (8) of [3]) for the former problem. We note, however, that a spheroid is a one-coordinate surface in prolate/oblate spheroidal coordinates. As an extension, we consider here a QD with a two-coordinate surface. The example that we have chosen is that of a lens-shaped QD in parabolic rotational coordinates (PRC). We will show that the mathematics has some similarity to the problem studied by Cantele *et al*; however, the two-coordinate surface leads to an additional level of complexity. Nevertheless, we were able to solve the problem exactly. Our structure is also of interest as regards investigating such effects as the influence of geometry on the energy spectrum, since the lens shape that we consider has a kink—as opposed to the spheroid. Hence, our structure is expected to be 'geometrically' closer to the flat lens grown experimentally. Some such studies of the energy dependence on shape and volume have already been reported [3, 9–11]. For example, Cantele *et al* and van Broek and Peeters both reported that the energy changed smoothly as a function of eccentricity for spheroidal and elliptical QDs, respectively, with the sphere having a minimum for the spheroidal problem [3] but not necessarily the circle for the ellipse problem [11]. As will be shown in section 3, we have obtained a completely different behaviour for the lens-shaped QD. Finally, the two-coordinate surface allows us to also study asymmetric QDs. Indeed, one can change the shape while keeping the volume constant by making the QD asymmetrical. One would, therefore, expect a stronger dependence of the energies on the shape.

In the next section, we show how Schrödinger's equation is separated using PRC and present two methods of solution of the resulting ordinary differential equations. We then present numerical results for various lens-shaped QDs.

2. Schrödinger's equation in parabolic rotational coordinates

In this section we show how to calculate the eigenfunctions and eigenvalues of an electron confined in a closed region of space defined by two paraboloids (figure 1). Such a surface can be described by two coordinates ξ and η which, together with a third coordinate ϕ, describe what is known as the PRC; the relationship to the Cartesian coordinates is as follows:

$$\begin{aligned} &x = \xi\eta\cos\phi, \qquad y = \xi\eta\sin\phi, \qquad z = \tfrac{1}{2}(\eta^2 - \xi^2), \\ &0 \leqslant \xi, \qquad \eta < \infty, \qquad 0 < \phi < 2\pi. \end{aligned} \tag{1}$$

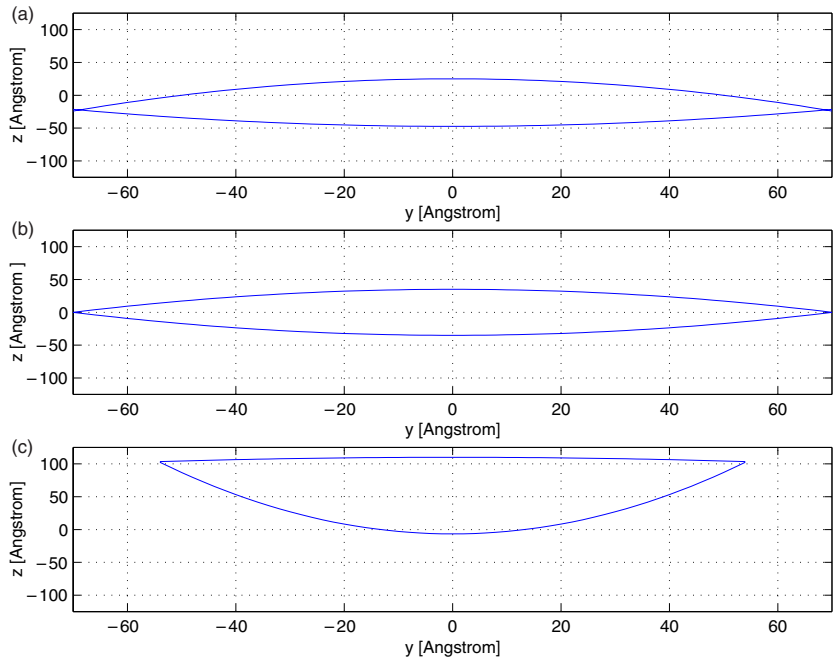

Figure 2. Various QDs of the same volume (yz-plane). The upper, middle, and lower figures correspond to the cases: (a) $\xi_0^2 = 50$ Å, (b) $\xi_0^2 = 70$ Å, and (c) $\xi_0^2 = 220$ Å, respectively. The QD volume is 5.39×10^5 Å^3.

The constant-ξ and constant-η surfaces are both paraboloids with respect to the positive and negative z-axes, respectively. $\xi = 0$ ($\eta = 0$) corresponds to the positive (negative) z-half-line. Note that ξ and η have the same domain; this is different from the case for the prolate spheroidal coordinates. While $\xi = \xi_0$ and $\eta = \eta_0$ are used to define a QD, more physically transparent parameters are the full height and radius (figure 1). The relationships of the various geometrical parameters are given as follows:

$$R = \xi_0 \eta_0, \tag{2}$$

$$h = \frac{\xi_0^2 + \eta_0^2}{2}, \tag{3}$$

$$V = \frac{\pi}{4} \xi_0^2 \eta_0^2 (\xi_0^2 + \eta_0^2) = \pi R^2 \frac{h}{2}, \tag{4}$$

where R, h, and V denote the radius, full height, and volume, respectively. The volume is obtained by integrating a volume element in PRC:

$$V = \int_0^{2\pi} \mathrm{d}\phi \int_0^{\eta_0} \mathrm{d}\eta \int_0^{\xi_0} \mathrm{d}\xi \, (\xi^2 + \eta^2) \xi \eta.$$

For the QDs depicted in figure 2, the volume is approximately 5.39×10^5 Å^3.

The bound states of an electron in the QD are obtained by solving Schrödinger's equation:

$$-\frac{\hbar^2}{2m^*} \nabla^2 \psi(\boldsymbol{r}) + V(\boldsymbol{r}) \psi(\boldsymbol{r}) = E \psi(\boldsymbol{r}), \tag{5}$$

with m^* the electron effective mass inside the QD, E the energy, ψ the wavefunction, and subject to the hard-wall boundary condition

$$\psi(\xi, \eta, \phi)|_{\xi=\xi_0, \eta=\eta_0} = 0. \tag{6}$$

Schrödinger's equation is known to be separable in PRC [12]. Writing

$$\psi(\xi,\eta,\phi) = M(\xi)N(\eta)\Phi(\phi), \tag{7}$$

one gets the following separated ordinary differential equations:

$$\frac{\mathrm{d}^2\Phi}{\mathrm{d}\phi^2} + k_3^2\Phi = 0, \tag{8}$$

$$\frac{1}{\xi}\frac{\mathrm{d}}{\mathrm{d}\xi}\left(\xi\frac{\mathrm{d}M}{\mathrm{d}\xi}\right) + \left[k_2 + k^2\xi^2 - \frac{k_3^2}{\xi^2}\right]M = 0, \tag{9}$$

$$\frac{1}{\eta}\frac{\mathrm{d}}{\mathrm{d}\eta}\left(\eta\frac{\mathrm{d}N}{\mathrm{d}\eta}\right) - \left[k_2 - k^2\eta^2 + \frac{k_3^2}{\eta^2}\right]N = 0, \tag{10}$$

where $k^2 = 2m^*E/\hbar^2$. The first equation, equation (8), is the familiar angular equation with solutions $\mathrm{e}^{\mathrm{i}p\phi}$, $p \in \mathcal{Z}$ when we impose periodic boundary conditions; hence, $k_3 = p$ (we will choose p positive since the $\pm p$ solutions are degenerate). The other two equations are known as the Bessel wave equations [13]. If $k = 0$, one recovers the Bessel equations. We now consider two methods for solving equations (9) and (10).

The first method, suggested by Zhang and Jin [14], involves a change of variables. First of all, let us rewrite the separation constants $k_2 = q^2$ (while k_2 can be negative, we will provide an efficient method for accounting for it without additional work) and $k_3^2 = p^2$. Then, equation (9) becomes

$$\frac{1}{\xi}\frac{\mathrm{d}}{\mathrm{d}\xi}\left(\xi\frac{\mathrm{d}M}{\mathrm{d}\xi}\right) + \left[q^2 + k^2\xi^2 - \frac{p^2}{\xi^2}\right]M = 0. \tag{11}$$

Now let

$$M(\xi) = \frac{V(v)}{\sqrt{v}}, \qquad \xi^2 = v. \tag{12}$$

Equation (11) becomes

$$\frac{\mathrm{d}^2V}{\mathrm{d}v^2} + \left[\frac{k^2}{4} + \frac{q^2}{4v} + \frac{1/4 - p^2/4}{v^2}\right]V = 0. \tag{13}$$

With a further substitution $v = z/(\mathrm{i}k)$, equation (13) becomes

$$\frac{\mathrm{d}^2V}{\mathrm{d}z^2} + \left[-\frac{1}{4} + \frac{\kappa}{z} + \frac{1/4 - \mu^2}{z^2}\right]V = 0, \tag{14}$$

where

$$\kappa = \frac{q^2}{4\mathrm{i}k}, \qquad \mu = \frac{p}{2}, \qquad z = \mathrm{i}kv = \mathrm{i}k\xi^2. \tag{15}$$

Equation (14) is known as Whittaker's equation [15]. Its solutions are known as the Whittaker functions [15]:

$$V(z) \equiv M_{\kappa,\mu}(z) = \mathrm{e}^{-z/2}z^{\mu+1/2}M(\tfrac{1}{2} + \mu - \kappa, 1 + 2\mu, z), \tag{16}$$

where $M(a,b,z)$ is a confluent hypergeometric function and is defined as

$$M(a,b,z) = 1 + \frac{az}{b} + \frac{(a)_2}{(b)_2}\frac{z^2}{2!} + \cdots + \frac{(a)_n}{(b)_n}\frac{z^n}{n!} + \cdots, \tag{17}$$

and $(a)_n \equiv a(a+1)\cdots(a+n-1)$. There is also a second solution that diverges logarithmically near the origin; we reject the latter solution on physical grounds. Finally, we can write down the solution to equation (11) as

$$M(\xi) = (\mathrm{i}k\xi^2)^{p/2}\mathrm{e}^{-\mathrm{i}k/2\xi^2}M\left(\frac{1}{2} + \frac{p}{2} - \frac{q^2}{4\mathrm{i}k}, 1 + p, \mathrm{i}k\xi^2\right), \tag{18}$$

where we have scaled $M(\xi)$ such that $M(\xi) = 1$ when $p = k = q = 0$ (to agree with the series solution to be derived later). Equation (18) is convenient since it relates the solution to a standard function, the confluent hypergeometric function. However, it poses some computational difficulties since there are both real and complex arguments. For instance, the extremely useful computer routines provided by Zhang and Jin [14] can only handle real arguments.

We have, therefore, directly derived a series solution to equation (11). This approach, known as the Frobenius method, was also used by Moon and Spencer [13]. The only singularity of equation (11) in the finite complex plane is a regular singular point at $\xi = 0$. Expanding the solution about $\xi = 0$, one writes

$$M(\xi) = \sum_{m=0}^{\infty} a_m \xi^{m+\sigma}. \tag{19}$$

If the differential equation is

$$x^2 y'' + x p(x) y' + q(x) y = 0,$$

with

$$p(x) = \sum_{m=0}^{\infty} p_m x^m, \qquad q(x) = \sum_{m=0}^{\infty} q_m x^m,$$

the indicial equation is

$$\Theta(\sigma) \equiv \sigma(\sigma - 1) + p_0 \sigma + q_0 = 0,$$

and the recurrence relation is

$$a_n = -\frac{\sum_{m=1}^{n} a_{n-m}[(\sigma + n - m) p_m + q_m]}{\Theta(\sigma + n)}.$$

In our case, we have

$$\sigma = \pm p, \tag{20}$$

$$a_n = -\frac{q^2 a_{n-2} + k^2 a_{n-4}}{(p+n)^2 - p^2}. \tag{21}$$

Here, p is an integer; hence, the indicial equation only leads to one independent solution (we will choose $\sigma = +p$ as the other solution diverges at $\xi = 0$). Choosing $a_0 = \frac{(q/2)^p}{\Gamma(p+1)}$, one obtains the series expansion of the Bessel wavefunction [13]:

$$M(\xi) = \frac{(q\xi/2)^p}{\Gamma(p+1)} \left\{ 1 - \frac{(q\xi/2)^2}{1!(p+1)} + \frac{(q\xi/2)^4}{2!(p+1)(p+2)} \left[1 - \frac{4(p+1)k^2}{q^4} \right] + \cdots \right\}$$
$$\equiv \mathcal{J}_p(k, q, \xi). \tag{22}$$

This series solution is easily amenable to numerical treatment. Furthermore, note that equation (22) is completely real. As a bonus, our two solutions, equations (18) and (22), allow us to obtain a relationship between the Bessel wavefunction and the Whittaker function:

$$\mathcal{J}_p(k, q, \xi) = \frac{(q/2)^p}{(\mathrm{i}k)^{p/2}\Gamma(p+1)} M_{q^2/(4\mathrm{i}k), p/2}(\xi). \tag{23}$$

This relation does not appear in the standard references on special functions [15–17].

The solution to equation (10) is obtained in a similar fashion to $M(\xi)$. Indeed, the recurrence relation, equation (21), applies with the change $q^2 \to -q^2$:

$$a_n = -\frac{-q^2 a_{n-2} + k^2 a_{n-4}}{(p+n)^2 - p^2}, \tag{24}$$

$$N(\eta) = \frac{(q\eta/2)^p}{\Gamma(p+1)} \left\{ 1 + \frac{(q\eta/2)^2}{1!(p+1)} + \frac{(q\eta/2)^4}{2!(p+1)(p+2)} \left[1 - \frac{4(p+1)k^2}{q^4} \right] + \cdots \right\}. \tag{25}$$

The hard-wall boundary condition (equation (6)) now becomes

$$M(k, q, p, \xi_0) = N(k, q, p, \eta_0) = 0, \tag{26}$$

where (ξ_0, η_0) defines the QD boundary. Equation (26) is solved by first specifying p (an integer). For each p, there remain two unknowns: k (related to the energy) and q, a separation constant. A simple procedure is to specify q and find the k-values for each function M and N to have zeros; the boundary condition is satisfied when the two values of q (and k) are identical.

It is possible for the separation constant k_2 in equations (9) and (10) to be negative (that is, of the form $k_2 = -q^2$). Instead of rederiving all the results to account for this case explicitly, we make use of the fact that equations (9) and (10) only differ in the sign of that same separation constant. Hence, given a (ξ_0, η_0) QD, one can find possible bound states for negative k_2 by instead finding the positive-k_2 solutions for the (η_0, ξ_0) QD. This result reflects the fact that the (ξ_0, η_0) QD and the (η_0, ξ_0) QD are just mirror images of each other in the xy-plane (they have the same radii, height, and volume as one can easily verify using equations (2)–(4)); hence, they have to have identical energy spectra.

3. Results and discussion

Two types of structure were studied: symmetrical and asymmetrical QDs. Symmetrical QDs are obtained when $\xi_0 = \eta_0$, when the plane of intersection of the two paraboloids is the $z = 0$ plane. When $\xi_0 \neq \eta_0$, the two surfaces have different curvatures. As a result, the intersection plane shifts vertically away from $z = 0$ (figure 2). In figure 2, three QD cross-sections in the yz-plane are shown. The three QDs are of the same volume (5.39×10^5 Å^3) with parameters $\xi_0^2 = 50$, 70, and 220 Å, respectively. For the symmetric QD, the radius and height are both 70 Å. The QDs have some basic spatial symmetries. They all have rotational and mirror symmetry about the z-axis; only the symmetric QDs have, in addition, a reflection plane ($z = 0$). The symmetry about the z-axis allows for twofold degeneracies. The reflection symmetry guarantees that the states of the symmetric QDs can be classified as even or odd about the $z = 0$ plane. From equations (22) and (25), one can deduce the following properties of the wavefunctions:

$$M(k = 0, q = 0, \xi) = N(k = 0, q = 0, \eta) = 1 \qquad (p = 0), \tag{27}$$

$$\psi(\xi = 0, \eta = 0, \phi) = 0 \qquad \forall p \neq 0. \tag{28}$$

The second equation implies that all the wavefunctions for nonzero p have at least one node (at the origin).

In searching for the energies, we started with q^2 and scanned in k for each of the two functions M and N that give zeros. The simultaneous zeros are the intersection points in a (q^2, k) plot. Examples for various QDs are shown in figure 3. Some actual values obtained for a symmetrical QD are given in table 1. A given bound state is, therefore, distinguished by three labels: p, q (or q^2), and k. p is equivalent to the azimuthal quantum number often labelled by m. Also, conventionally, instead of k, one uses the counting index of k and labels it by n, the principal quantum number; we will also do so here. However, q does not have a direct analogue. Furthermore, it is non-integral and complex. Hence, we have decided to fold it into n; i.e., n counts the number of distinct (q^2, k) pairs in increasing order of energy (for each p).

The lowest calculated energies for two structures are given in table 2. For all the calculations, we used the effective mass of GaAs, $m^* = 0.067\, m_0$. Referring to the symmetric QD first, the ordering of levels is $(n, p) = (1, 0) < (1, 1) < (1, 2) < (2, 0) < \cdots$. The energy of the ground state, 0.268 eV, is obviously larger than, for example, that of a cylinder

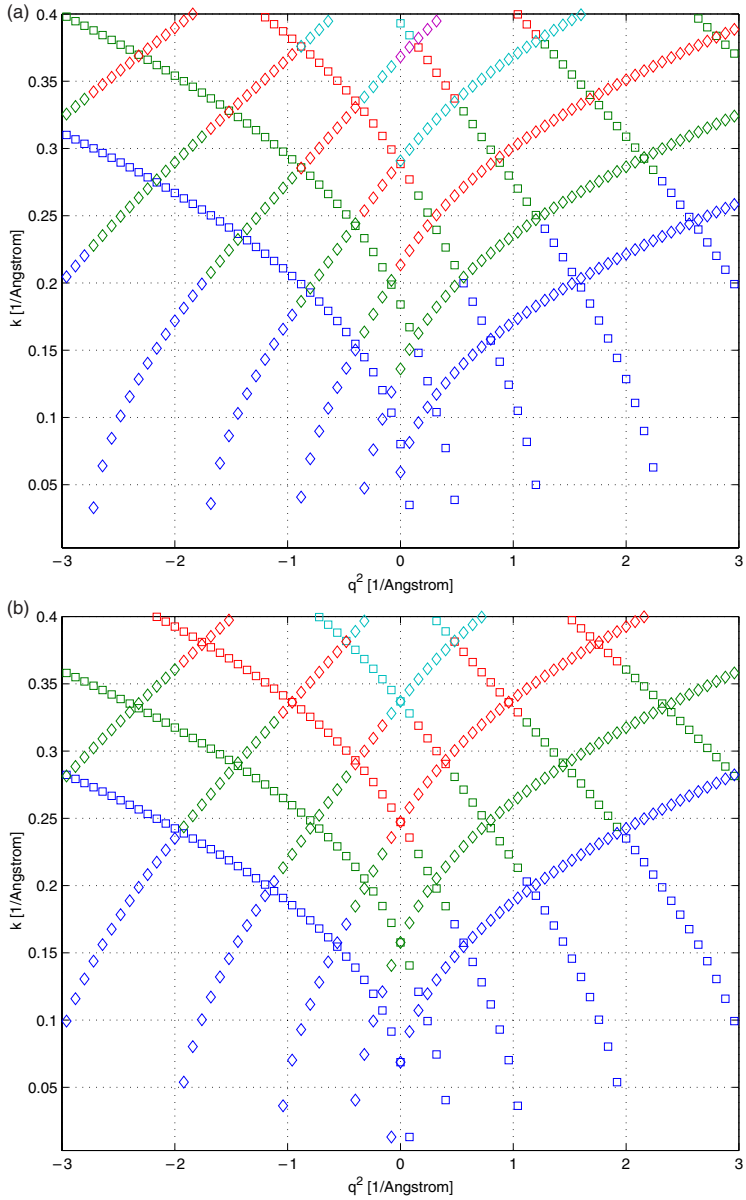

Figure 3. Plots of k versus q^2 for two QDs with the same volume ($p = 0$). The figures correspond to the cases: (a) $\xi_0^2 = 70$ Å, $\eta_0^2 = 70$ Å; and (b) $\xi_0^2 = 60$ Å, $\eta_0^2 = 81.1$ Å. The QD volume is 5.39×10^5 Å^3.

with the same radius and full height, the ground state energy of the latter being 0.182 eV. The meanings of the quantum numbers n and p are similar to, for example, the elliptical dot [11]. Thus they relate to the nodal structure in the radial and ϕ-directions. This is evident in the wavefunctions plotted in the xy-plane at $z = 0$ (figure 4). It was verified numerically that the absolute value of the wavefunction at the rim of the QD is less than 10^{-7} as compared to the its maximum value for all the states shown. We have also given the contour plot of the (2, 0)

Table 1. Lowest (q^2, k) values for a symmetrical QD ($\xi_0^2 = \eta_0^2 = 70$ Å).

p	q^2 (Å^{-1})	k (Å^{-1})
0	0.0	0.0687, 0.1577, 0.2473
	0.191	0.1122
		⋮
1	0.0	0.0898

Table 2. Energies (in eV) for a symmetrical and an asymmetrical lens-shaped QD (using $m^* = 0.067\, m_0$). The $q = 0$ solutions are given in bold.

	$\xi_0^2 = 70$ Å, $\eta_0^2 = 70$ Å			$\xi_0^2 = 90$ Å, $\eta_0^2 = 53.2$ Å		
n	$p = 0$	$p = 1$	$p = 2$	$p = 0$	$p = 1$	$p = 2$
1	**0.268**	**0.458**	**0.682**	0.265	0.450	0.682
2	0.712	1.01	1.34	0.671	0.967	1.29
3	1.37	1.78	2.20	0.739	1.04	1.39
4	**1.43**	**1.83**	**2.28**	1.28	1.66	2.07
5	2.23	2.72	3.26	1.38	1.81	2.27

and (4, 0) states in a ϕ-plane (figure 5). The number of features is a reflection of the excited nature of these states. The interesting difference is that the (4, 0) state is symmetric about the $z = 0$ plane but the (2, 0) state has no such symmetry. Indeed, the only states that display such a symmetry must have $q = 0$, which also implies that these states are either even or odd. One can, in fact, prove that only the even states are allowed. In order to demonstrate this, we need the inverse of the coordinate equations in equation (1). In the zx-plane, we have

$$\xi = \left[-z + \sqrt{z^2 + x^2}\right]^{1/2}, \tag{29}$$

$$\eta = \left[z + \sqrt{z^2 + x^2}\right]^{1/2}. \tag{30}$$

Note that ξ and η go into each other under the $z \to -z$ transformation. Looking at equations (22) and (25), one notes that the solutions can therefore be rewritten in the form

$$M(x, 0, z) = \sum_n a_n \left[-z + \sqrt{z^2 + x^2}\right]^n, \tag{31}$$

$$N(x, 0, z) = \sum_n b_n \left[z + \sqrt{z^2 + x^2}\right]^n, \tag{32}$$

with the a_n only equal to b_n for all n if $q = 0$. When that is the case,

$$\psi(x, 0, -z) = M(\xi')N(\eta') = N(\eta)M(\xi) = \psi(x, 0, z). \tag{33}$$

Hence the state is even. When $q \neq 0$, no such symmetry exists in our solutions. However, this is due to the double degeneracy of these states (with respect to the sign of q^2, as is evident in figure 3(a)). Indeed, we know already that M and N get interchanged upon sign change of q^2 and the two solutions that we have obtained are mirror images of each other with respect to the $z = 0$ plane. This also explains why the $q = 0$ states are all even. Recalling the degeneracy with respect to the sign of p, we therefore have the following degeneracies for the first few states of the symmetric lens-shaped QD (in order of increasing energy): 1 (ground state), 2, 2, 2, 4, ... Note that there are other states beyond the ground state that are nondegenerate. For

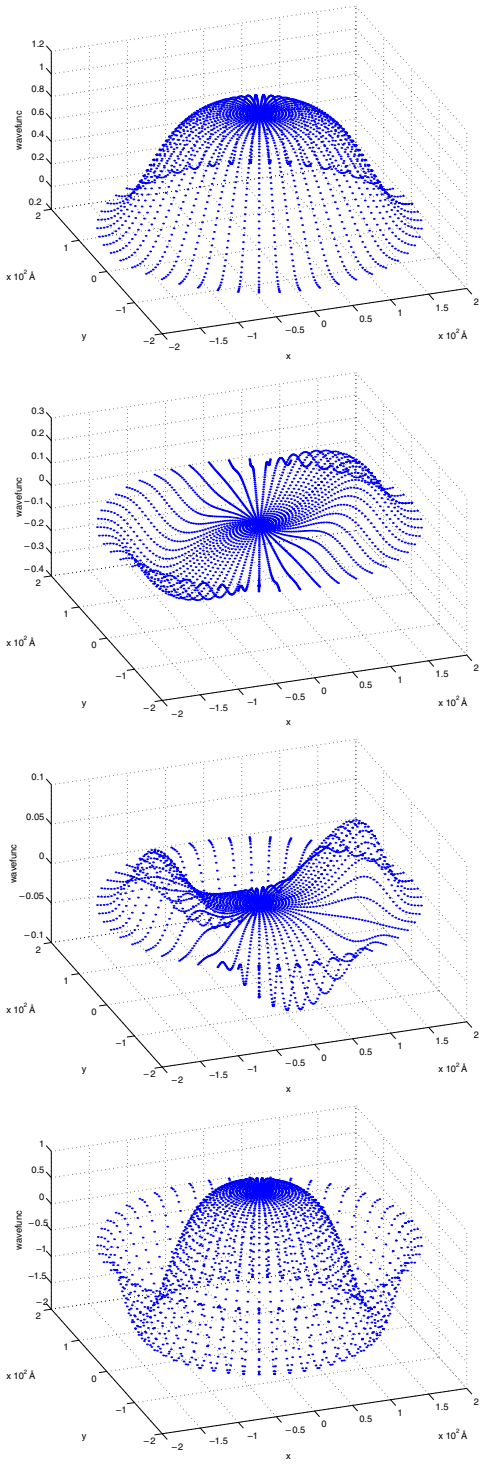

Figure 4. Plots of the first four wavefunctions in the xy-plane (for $z = 0$) for the symmetrical QD.

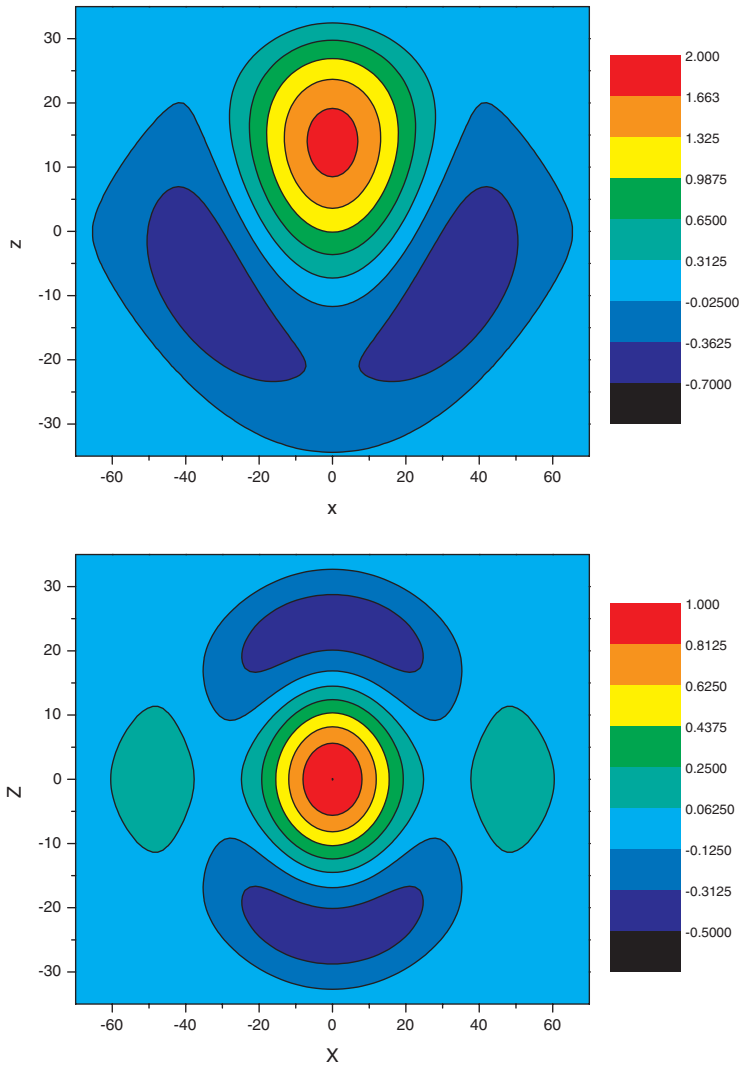

Figure 5. Contour plots in the zx-plane (for $y = 0$) of the (2, 0) and (4, 0) states for the symmetrical QD.

example, the (4, 0) state that we have already studied is nondegenerate. On the other hand, no degeneracies higher than four are expected.

For the asymmetric structure, we have chosen one with the same volume as and slightly smaller radius than the symmetric one but with a larger height. It is evident that asymmetry leads to lower state energies for all p-values considered. The energies for the bound state of the asymmetric QD can be understood with reference to figure 3. The k versus q^2 plots for the symmetric structure ((a) $\xi_0^2 = 70$ Å; $\eta_0^2 = 70$ Å), and one asymmetric structure ((b) $\xi_0^2 = 60$ Å; $\eta_0^2 = 81.1$ Å), are shown in the top and bottom figures, respectively. The ground state energy for the symmetric structure is at $(q^2, k) = (0, 6.87 \times 10^{-2}\ \text{Å}^{-1})$ corresponding to $E = 0.268$ eV. This point is the smallest value in k where crossing of the curves occurs such that equation (26) is fulfilled. Crossings happen exactly at $q = 0$, as the recurrence

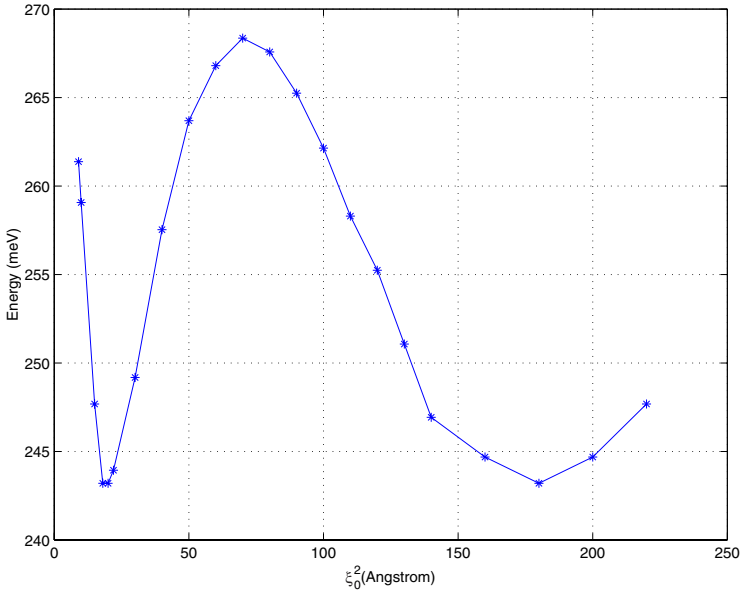

Figure 6. The ground state energy for various QDs of the same volume. The volume is the same as for figure 3.

relations for M and N are identical in this case. Thus, $M(\xi_0) = N(\eta_0)$ if $\xi_0 = \eta_0$ and $q = 0$. However, if $\xi_0 > \eta_0$ (even by a small amount) the lowest crossing occurs for $q^2 < 0$ as shown in the bottom figure. For example, the ground state of the $(\xi_0^2, \eta_0^2) = (90, 53.2)$ QD has $(q^2, k) = (-0.0342, 0.0225)$. The k-value is seen to be smaller than the corresponding one for the symmetrical QD—hence the lower energy. As already pointed out, the same spectrum is obtained if ξ_0 is slightly smaller than η_0, instead of slightly bigger.

We have investigated the shape dependence of the energy spectrum at constant volume in more detail. This was done for numerous volumes. Figure 6 shows the ground state energy as a function of the ξ_0^2-value for a series of QDs having the same volume as before (5.39×10^5 Å^3). A similar study was performed by Cantele *et al* [3] as they went from a spherical dot to a spheroidal one. They did the calculations for volumes of spheroids similar to the volume of our QDs. A similar study in two dimensions was performed by von Broek and Peeters [11] going from an ellipse to a circle (however, the latter work is quantitatively incorrect since the finite-barrier problem is not separable as they assumed). The energy is seen to have a maximum for the symmetric QD sandwiched between two minima. This differs from the results obtained by Cantele *et al* [3] where the symmetric structure has a lower energy. Hence, this indicates that the dependence of the ground state energy on shape is not universal. Indeed, the difference between the result of Cantele *et al* and ours is readily explainable. In their case, the 'symmetric' structure is spherical and any distortion into a spheroid corresponds to an 'elongation' or stretching of the structure. In our case, the starting symmetrical QD has a rather flat shape in the z-direction (lens shaped; figure 2(b)). The subsequent distortion (by stretching one coordinate surface in the z-direction) leads to a less flat shape (figure 2(a))—hence the drop in the energy. However, for larger distortion still, one of the two surfaces is now almost flat (figure 2(c)), squeezing the wavefunction in the process, and the energy therefore starts going up again. It is also interesting that the shape of the QD (figure 2(c)) now approximates a flat lens [8]. We have repeated our calculations for a much larger volume

(about 1.0×10^7 Å^3 which, for the symmetric QD, corresponds to a lens-shaped QD of radius 200 Å), since many of the QDs being grown have volumes larger than the ones considered by Cantele *et al* [3]. For these larger volumes, we found smaller dependence of the ground state energy on the shape, as expected. Thus, shape might not be so important for these QDs.

4. Summary

The problem of infinite-barrier lens-shaped QDs in PRC has been solved exactly. This has allowed us to obtain a new relation connecting the Bessel wavefunctions to the Whittaker functions. Energies and wavefunctions are given for symmetrical and asymmetrical QDs. It was found that the ground state energy is very sensitive to the shape of the QD at constant volume only for small volume. The degeneracy of the energy spectrum was also worked out.

Acknowledgments

We thank Calin Galeriu for helpful discussions. We also thank one of the referees for an insightful comment regarding figure 6. This work was supported by an NSF CAREER award (NSF Grant No 9984059).

References

[1] Bimberg D, Grundmann M and Ledentsov N N 1999 *Quantum Dot Heterostructures* (New York: Wiley)
[2] Grundmann M, Stier O and Bimberg D 1995 *Phys. Rev.* B **52** 11969
[3] Cantele G, Ninno D and Iadonisi G 2000 *J. Phys.: Condens. Matter* **12** 9019
[4] Efros Al L and Efros A L 1982 *Sov. Phys.–Semicond.* **16** 772
[5] Marzin J Y and Bastard G 1994 *Solid State Commun.* **92** 437
[6] Lew Yan Voon L C and Willatzen M 1995 *Semicond. Sci. Technol.* **10** 416
[7] Le Goff S and Stébé B 1993 *Phys. Rev.* B **47** 1383
[8] Wojs A, Hawrylak P, Fafard S and Jacak L 1996 *Phys. Rev.* B **54** 5604
[9] Efros Al L and Rodina A V 1993 *Phys. Rev.* B **47** 10005
[10] Pryor C 1999 *Phys. Rev.* B **60** 2869
[11] van den Broek M and Peeters F M 2001 *Physica* E **11** 345
[12] Morse P M and Feshbach H 1953 *Methods of Theoretical Physics* (New York: McGraw-Hill)
[13] Moon P and Spencer D E 1961 *Field Theory Handbook* (Berlin: Springer)
[14] Zhang S and Jin J 1996 *Computation of Special Functions* (New York: Wiley)
[15] Abramowitz M and Stegun I A 1970 *Handbook of Mathematical Functions* (New York: Dover)
[16] Watson G N 1958 *A Treatise on the Theory of Bessel Functions* (Cambridge: Cambridge University Press)
[17] Erdélyi A, Magnus W, Oberhettinger F and Tricomi F G 1953 *Higher Transcendental Functions* (New York: McGraw-Hill)